Current-climate sea ice amount and seasonality as constraints for future Arctic amplification

ENVIRONMENTAL RESEARCH
CLIMATE

OPEN ACCESS

RECEIVED
13 April 2023

REVISED
21 August 2023

ACCEPTED FOR PUBLICATION
29 August 2023

PUBLISHED
18 September 2023

PAPER

Current-climate sea ice amount and seasonality as constraints for future Arctic amplification

Olivia Linke[1,*], **Nicole Feldl**[2] and **Johannes Quaas**[1]

[1] Leipzig Institute for Meteorology, Leipzig University, Leipzig, Germany
[2] Department of Earth and Planetary Sciences, University of California Santa Cruz, Santa Cruz, CA, United States of America
[*] Author to whom any correspondence should be addressed.

E-mail: olivia.linke@uni-leipzig.de

Keywords: Arctic amplification, Arctic sea ice, Climate feedbacks, emergent constraints, CMIP6, climate change

Abstract

The recent Arctic sea ice loss is a key driver of the amplified surface warming in the northern high latitudes, and simultaneously a major source of uncertainty in model projections of Arctic climate change. Previous work has shown that the spread in model predictions of future Arctic amplification (AA) can be traced back to the inter-model spread in simulated long-term sea ice loss. We demonstrate that the strength of future AA is further linked to the current climate's, observable sea ice state across the multi-model ensemble of the 6th Coupled Model Intercomparison Project (CMIP6). The implication is that the sea-ice climatology sets the stage for long-term changes through the 21st century, which mediate the degree by which Arctic warming is amplified with respect to global warming. We determine that a lower base-climate sea ice extent and sea ice concentration (SIC) in CMIP6 models enable stronger ice melt in both future climate and during the seasonal cycle. In particular, models with lower Arctic-mean SIC project stronger future ice loss and a more intense seasonal cycle in ice melt and growth. Both processes systemically link to a larger future AA across climate models. These results are manifested by the role of climate feedbacks that have been widely identified as major drivers of AA. We show in particular that models with low base-climate SIC predict a systematically stronger warming contribution through both sea-ice albedo feedback and temperature feedbacks in the future, as compared to models with high SIC. From our derived linear regressions in conjunction with observations, we estimate a 21st-century AA over sea ice of 2.47–3.34 with respect to global warming. Lastly, from the tight relationship between base-climate SIC and the projected timing of an ice-free September, we predict a seasonally ice-free Arctic by mid-century under a high-emission scenario.

1. Introduction

The Arctic region experiences a particularly high susceptibility to climate change. In recent decades, the northern high latitudes have warmed faster than the globe, which is seen in both observations (Serreze and Francis 2006, Serreze *et al* 2009, Screen and Simmonds 2010, Polyakov *et al* 2012, Cohen *et al* 2014, Wendisch *et al* 2023) and model simulations (Holland and Bitz 2003, Stroeve *et al* 2012, Wang and Overland 2012). This Arctic amplification (AA) of climate change has strong implications for natural and human systems also beyond the Arctic boundary (Overland *et al* 2016, Francis *et al* 2017) which highlights the need to correctly predict its strength. Although state-of-the-art climate models agree on the sign of AA, they project a considerable range in its magnitude.

Primarily local mechanisms that act on regional scales have been suggested to give rise to this inter-model spread (Boeke and Taylor 2018). It is well established that the substantial Arctic sea ice loss and the associated sea-ice albedo feedback (SIAF) are of central importance in giving rise to AA (Hall 2004, Screen and Simmonds 2010, Graversen *et al* 2014), which is expected to continue under advancing global warming (Stroeve *et al* 2012). The long-term loss of sea ice exposes more open ocean with a lower albedo, which leads

to stronger solar absorption and ocean heat storage in summer. The anomalously stored heat is transferred to fall / winter and released to the atmosphere, which amplifies surface warming and hampers freeze up (Hall 2004, Serreze and Barry 2011, Goosse *et al* 2018). It is thereby implied that the spread in climate-model projections of AA is linked to the variable degree by which models simulate long-term sea ice loss. In particular, it has been pointed out that models with stronger decadal sea ice loss systematically produce greater AA, which suggests a negative relationship between changes in sea ice amount and AA (Holland and Bitz 2003, Boeke and Taylor 2018, Dai *et al* 2019).

In addition, earlier work highlights the importance of the initial sea ice climatology for the evolution of Arctic warming. Holland and Bitz (2003) found that in CMIP2 models, the sea ice extent is systematically related to Arctic warming and AA under CO_2-driven climate change. In particular, they show a negative correlation between the latitude of maximum warming and initial sea ice extent across models. In the seasonal context and specifically for the SIAF, Thackeray and Hall (2019) demonstrate a positive correlation across CMIP5 models between the future SIAF and its seasonal feedback analogue that occurs during spring and summer ice melt. In other words, the sensitivity of ice across the base state's seasonal cycle determines its sensitivity to projected warming.

Here, we thoroughly examine the link between the magnitude of future AA throughout the 21st century and the sea ice climatology of the current climate state. In particular, we explore the sensitivity of AA to base-climate Arctic sea ice amount, as quantified by sea ice extent and average sea ice concentration (SIC) (percentage by which the Arctic ocean is covered by sea ice). Firstly, we argue that the model spread in simulated sea-ice loss is linked to the model spread in base-climate sea-ice amount across models. In other words, the amount of sea ice in the current climate sets the stage for the degree of future climatological changes that mediate the strength of AA. Secondly, we examine if the magnitude of future AA is tied to the current climate's seasonal cycle in Arctic sea ice, i.e. the difference between seasonal ice maximum and minimum.

To understand the physical mechanisms at play, we explore the connection between initial sea ice amount and those climate feedbacks that are known to substantially contribute to the local amplification of climate change in the Arctic. Those are, besides the SIAF, the two longwave temperature feedbacks (Pithan and Mauritsen 2014): The Planck feedback contributes to AA given that at colder temperature (i.e. in the polar regions), the atmosphere experiences a smaller increase in emitted blackbody radiation per unit warming. The lapse-rate feedback (LRF) arises from the vertically non-uniform warming, which constitutes a positive feedback the Arctic, while being slightly negative on global average (Block and Mauritsen 2013, Pithan and Mauritsen 2014, Goosse *et al* 2018, Feldl *et al* 2020, Hahn *et al* 2021).

We explore the link between sea ice climatology, feedbacks and AA through linear regressions in the Coupled Model Intercomparison Project phase 6 (CMIP6) ensemble. For robust linear relationships at the 95% level, we propose an emergent constraint (EC), a framework for characterizing strong statistical and physically explainable relationships between observable aspects of the current climate and future simulations across climate models (Klein and Hall 2015, Hall *et al* 2019, Thackeray and Hall 2019). Our attempt is to narrow the spread in future Arctic climate projections by predicting the evolution of AA through the 21st century, based upon the current climate's sea ice climatology.

2. Data and methods

2.1. CMIP6 simulations

We consider model output data from 30 CMIP6 climate models that provide monthly diagnostics for near-surface air temperature and required sea ice metrics. The model subset is specified in table 1. We use model output data for the time period 2005–2099 which combines diagnostics from the historical (2005–2014) and the scenario simulations (2015–2099), using each model's first realization. The climate change scenario assumes the highest emission pathway SSP5-8.5 (O'Neill *et al* 2016). The base period as an estimate of the current climate state is chosen as the 30-year period centered around the year 2019 (2005–2034). We hereby find a compromise between including sufficient years in the observational data sets (2016–2022; also centered around 2019) and allowing a constraint on AA through the 21st century, without emergent relationships breaking down. Moving the base period further into the recent past (e.g. 2008–2022) would enable the inclusion of more observational data, but leads to a statistical degrading of linear relationships. We note that by choosing a base period that cannot be fully covered by the observations, an error might occur when constraining AA. We therefore test the similarity between simulated sea ice metrics for the model base period (2005–2034), and the observational base period (2016–2022). Under the assumption of an approximately linear sea ice loss, the average of simulated sea ice metrics for both periods should be approximately the same. We further elaborate on that later in the discussion.

Table 1. List of CMIP6 models used in this study.

Model	Reference
ACCESS-CM2	Dix *et al* (2019)
ACCESS-ESM1-5	Ziehn *et al* (2019)
BCC-CSM2-MR	Xin *et al* (2019)
CAMS-CSM1-0	Rong (2019)
CESM2 [a]	Danabasoglu (2019)
CIESM [a]	Huang (2019)
CMCC-CM2-SR5 [a]	Lovato and Peano (2020)
CMCC-ESM2 [a]	Lovato *et al* (2021)
CNRM-CM6-1	Voldoire (2019)
CNRM-CM6-1-HR	Voldoire (2019)
CanESM5 [a]	Swart *et al* (2019)
CanESM5-CanOE [a]	Swart *et al* (2019)
EC-Earth3	EC-Earth Consortium (2019)
EC-Earth3-CC	EC-Earth Consortium (2021)
EC-Earth3-Veg	EC-Earth Consortium (2019)
EC-Earth3-Veg-LR	EC-Earth Consortium (2020)
FIO-ESM-2-0 [a]	Song *et al* (2019)
GFDL-CM4	Guo *et al* (2018)
GFDL-ESM4	John *et al* (2018)
GISS-E2-1-G	NASA/GISS (2020)
HadGEM3-GC31-LL	Good (2019)
HadGEM3-GC31-MM	Jackson (2020)
IPSL-CM6A-LR	Boucher *et al* (2019)
MIROC-ES2L	Tachiiri *et al* (2019)
MPI-ESM1-2-HR [a]	Schupfner *et al* (2019)
MRI-ESM2-0 [a]	Yukimoto *et al* (2019)
NESM3 [a]	Cao (2019)
NorESM2-LM	Seland *et al* (2019)
NorESM2-MM	Bentsen *et al* (2019)
UKESM1-0-LL	Good *et al* (2019)

[a] Excluded for constraining the prediction range of the 21st-century AA.

2.1.1. Arctic amplification

AA can be defined as the ratio of linear-trend slopes of Arctic and global-mean temperature change (Smith *et al* 2019, Rantanen *et al* 2022):

$$\mathrm{AA} = \frac{\mathrm{d}T_{\mathrm{s,Arctic}} / \mathrm{d}t}{\mathrm{d}T_{\mathrm{s,Globe}} / \mathrm{d}t}. \tag{1}$$

The linear trends of near-surface air temperature $\mathrm{d}T_{\mathrm{s}} / \mathrm{d}t$ for the specific regions are calculated using a least-squares fitting for the annual mean values, for the period 2005–2099. As an alternative, AA can be derived as the ratio of Arctic and global warming, with warming being defined as the difference between the average temperature during 2070–2099 and the base period. However, both methods produce highly similar results (not shown explicitly), which is why we stick to the ratio of the warming trend in the Arctic to the global-mean.

Our constraint on AA concerns the area north of the Arctic boundary, here defined at 66° N latitude (NH66 domain). We further exclude land masses and areas of open ocean in each model's current climatology to reduce their weakening impact on the relationship between AA and sea ice cover in the base climate. This is motivated not only by the stronger correlation, as expected when focusing on the same area for both variables, but also by the physical underpinning of AA being largely tied in magnitude to sea ice loss (Dai *et al* 2019). Therefore, our main results focus on the locally amplified surface warming as averaged over the Arctic ocean area covered by sea ice in the current climate. However, we also consider in the discussion the effect of including open-ocean areas in the base climate on the prediction range of future AA.

2.1.2. Sea ice metrics

To estimate the sea ice amount in the current climate and its evolution through the century, we consider annual-mean model diagnostics of sea ice concentration and derived sea ice extent (SIE). The SIC gives the percentage of model grid cell area covered by sea ice. We apply a threshold of 15% above which a grid cell is classified as sea ice. Our derived Arctic-mean values of SIC give an overall estimate of the percentage of ice covering the Arctic ocean north of 66° N latitude. The SIE is calculated as the total area of all model grid cells

above the threshold of 15% SIC (Notz and SIMIP Community 2020). We consider the SIE spanning the Northern Hemisphere (NH), not only the NH66 domain, as ice covers nearly the entire NH66 region in the current climate.

Therefore, the SIE gives an area metric for the model-specific ice cover, whereas the area-average SIC gives an estimate of the fractional ice coverage spanning that particular area.

2.1.3. Climate feedbacks

To examine the role of climate feedbacks and their connection to both base-climate sea ice metrics and future AA, we compute the magnitude of three climate feedbacks that largely contribute to AA.
These are the SIAF and the longwave temperature feedbacks.

The feedbacks are derived from a pre-computed radiative kernel which gives the change in top-of-the-atmosphere radiation balance due to a perturbation in an atmospheric state variable (for the temperature feedbacks that is 1 K, for the SIAF it is 1% of surface albedo, respectively). We consider the radiative kernel from the HadGEM3-GA7 climate model (Smith *et al* 2020).

We derive warming contributions for the SIAF, LRF, and the variation in the Planck response from its global-mean value (PR') using the local energy budget equation as in prior studies (Feldl and Roe 2013, Taylor *et al* 2013, Pithan and Mauritsen 2014, Goosse *et al* 2018). The feedback warming is thereby calculated as contribution to the end-of-century Arctic warming (2070–2099) over Arctic ocean covered with sea ice in the current climate (as for AA).

2.2. Satellite observations

We use SIC satellite data that is provided by the European Organisation for the Exploitation of Meteorological Satellites (EUMETSAT) Ocean and Sea Ice Satellite Application Facility (OSI SAF) (Lavergne *et al* 2019). As for the model diagnostics, the observed SIE is derived by summing all grid cells with SIC values above 15% over the NH.

3. Results

3.1. Current-climate sea ice amount and seasonally ice-free Arctic

CMIP6 models project a considerable spread in base-climate SIC on an Arctic mean scale (figure 1). The simulations show that between 60%–90% of the Arctic ocean north of the 66° N latitude is covered by sea ice in the current climate across 30 CMIP6 models. The inter-model spread in SIC is positively correlated to the simulated spread in SIE across all 30 models ($r = 0.88$, not shown), with values ranging from 6.2–14.6 $\times 10^6$ km^2. We expect this inter-model spread in projected current-climate sea ice amount to relate to the magnitude of future-climate AA.

Similarly to Thackeray and Hall (2019), we find that our derived relationships substantially degrade when including models with the lowest sea ice amount in the base climate (in their study quantified by sea-ice thickness). We adapt this approach and remove models with unrealistically low SIC (and SIE) in the base-climate (10 models in our case). This leaves us with an ensemble of 20 models that project an area-average SIC of 75% or more in the base climate (marked in figure 1). This matter is further explained in the discussion, and we repeat the EC analysis for all 30 models in appendix C.

Figure 1 suggests a strong correlation ($r = 0.95$) between base-climate SIC and predicted year of the first ice-free September. From the uncertainty range around the observational estimate, we derive a constraint on the timing of a seasonally ice-free Arctic by mid-century (2038–2059).

3.2. 21st-century Arctic amplification

Out of the CMIP6 ensemble, 20 models are considered for the derivation of linear relationships between current sea ice state and future AA. Those models simulate a considerable range in magnitude of AA: figure 2 shows maps of the amplification factor of local and annual-mean warming relative to the global average. Corresponding to equation (1), the local amplification is derived as the ratio of near-surface warming trend per model grid cell, $\mathrm{d}T_s / \mathrm{d}t$, and global-mean warming trend $\mathrm{d}T_{s,\,\mathrm{Globe}} / \mathrm{d}t$ during 2005–2099.

For all models and the model average, the NH66 domain comprises the hotspot of local amplification over the ice covered ocean. Arctic land masses show lower values, compared to the ice cover of the base climate. Open ocean areas are almost not present in the NH66 region, but in lower latitudes they show an amplification factor less than 1 across all models. Therefore, open ocean areas warm less in relation to the global average which is linked to ocean heat uptake (Huguenin *et al* 2022).

Despite all models agreeing on an amplification of global warming in the Arctic, the inter-model spread is large, and strong spatial variations occur across the CMIP6 ensemble. The spread among climate model

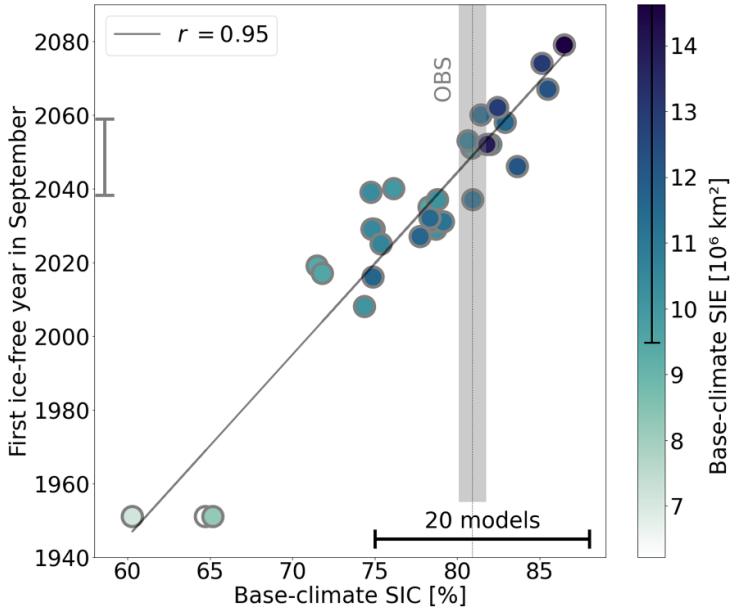

Figure 1. Inter-model relationship between base-climate sea ice amount and the timing of an ice-free Arctic: relationship between annual-mean SIC and first year with ice-free September. The correlation ($r = 0.95$) is statistically significant at the 95% level. The first ice-free September is defined as the year where the SIE is below 1×10^6 km^2. Each model is denoted by a circle, color coded by the annual-mean SIE in the base-climate. The mean observational estimate (2016–2022) of SIC is shown by the grey dotted line, with grey shaded areas giving ± 1 of the inter-annual standard deviation. The black bar along the x-axis marks the SIC range of those 20 models considered for an EC. The corresponding range in SIE is marked in the color bar.

predictions is largest over the ice-covered Arctic ocean, primarily over the strong future ice-melt regions of the Barents-Kara-sea (figure A1 shows the spatial pattern of the inter-model standard deviation).

The next section explores the spread in future AA projections and its link to the simulated spread in the current climate's sea ice climatology. In conjunction with observations, emerging relationships allow for an evaluation of model suitability for simulating future Arctic climate change.

3.3. Emergent constraint on Arctic amplification

In figure 3 we derive significant linear correlation coefficients between the magnitude of the 21st-century AA and current-climate SIE, SIC, as well as sea ice seasonality across 20 CMIP6 models. We consider the SIE of the entire NH, and SIC as the averaged value over the NH66 domain. The seasonality is derived as the amplitude of the seasonal cycle of SIC (figure 4).

In our first hypothesis, we proposed that the magnitude of future AA through the 21st century is sensitive to the current climate's sea ice amount. As pointed out before, CMIP6 models show a large spread in initial sea ice amount, quantified by both Arctic-mean SIC and SIE during 2005–2034. Figure 3(a) shows that models with lower base-climate SIE simulate a stronger 21st-century AA ($r = -0.70$). In addition, a lower SIE systematically relates to a lower SIC across models (figure B1(a); $r = 0.79$). Therefore, models with smaller SIE also simulate a lower Arctic-mean ice-cover percentage. The smaller SIC over the Arctic ocean corresponds to a stronger future AA ($r = -0.77$; figure 3(b)). This is due to lower initial SIC enabling stronger ice loss throughout the century: figure B1(b) shows that base-state SIC and long-term changes in SIC ongoing from the base period, are positively correlated ($r = 0.82$). Consequently, stronger ice loss mediates stronger AA throughout the century ($r = -0.87$; figure B1(c)).

In a second hypothesis, we suggested that the magnitude of future AA is linked to the seasonal cycle of Arctic sea ice in the base period. The seasonal cycle of SIC is depicted in figure 4: All models show seasonal variations, with the SIC maximum during February–March–April (FMA), and SIC minimum during July–August–September (JAS). The seasonality is derived as the amplitude of the seasonal cycle of SIC ($SIC_{FMA} - SIC_{JAS}$). It is further evident that those models with lower annual-mean base-period SIC project a stronger seasonal cycle in the base period ($r = -0.86$; figure B1(d)). Figure 3(c) shows that a stronger sea-ice seasonal cycle in the current climate is linked to stronger future AA across models ($r = 0.73$). In other words, models with more intense seasonal ice melt and growth project a stronger AA throughout the 21st century.

From the range of observational estimates for SIE, SIC, and $SIC_{FMA} - SIC_{JAS}$ in conjunction with the emerging linear relationships, a prediction interval of future AA can be derived. On the basis of figure 3 we

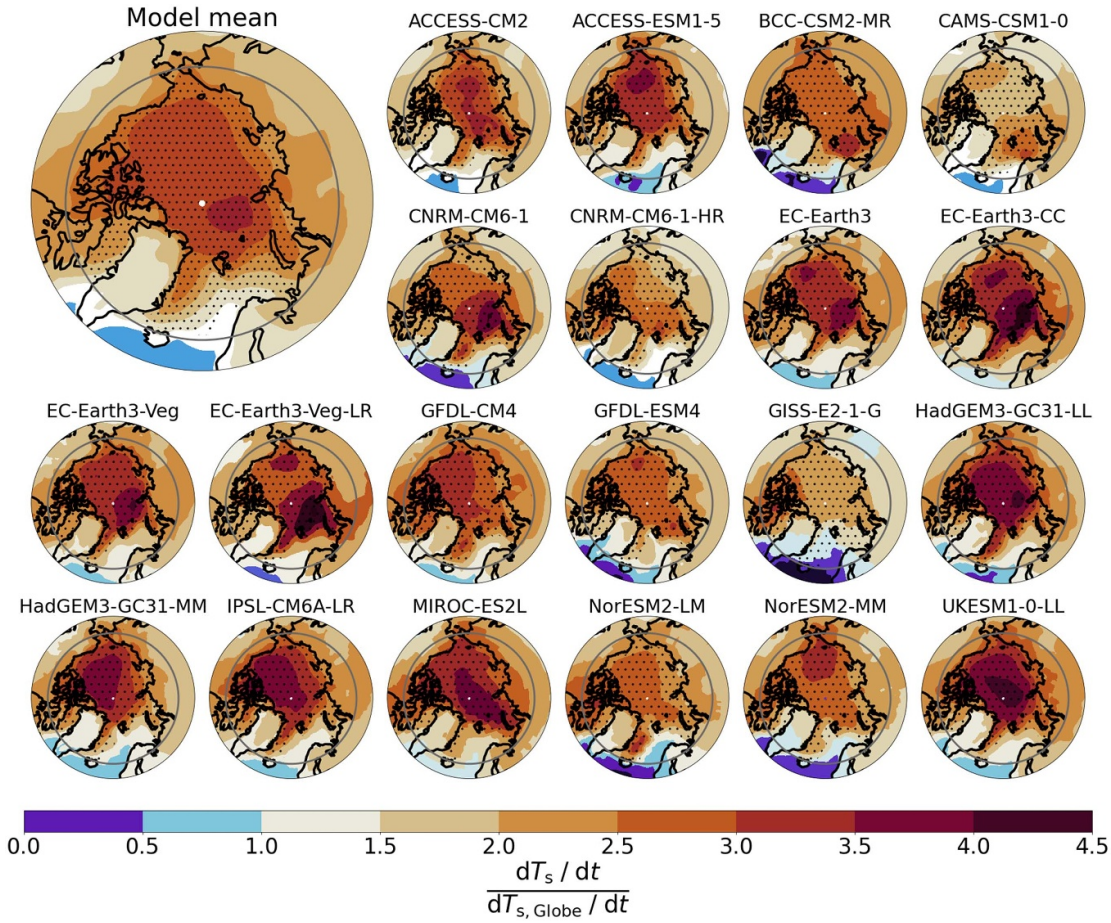

Figure 2. Maps of 21st-century Arctic warming, as local amplification factor: ratio of local warming trend dT_s / dt and global-mean warming trend $dT_{s,\,Globe} / dt$ during 2005–2099. Values larger than 1 account for a locally amplified warming with respect to global warming, and thereby a positive contribution to AA. The ice covered ocean in the base climate is marked by the dotted areas for each model and the model mean. The NH66 domain is marked by the grey circle.

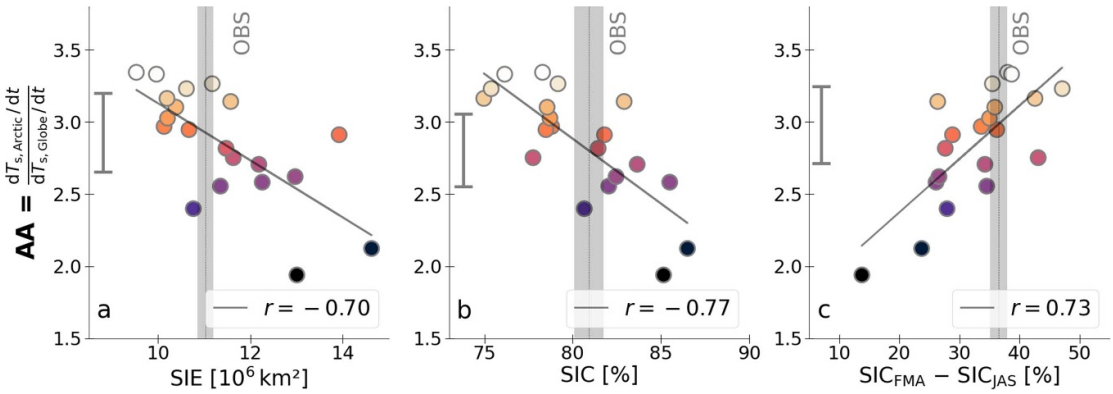

Figure 3. Inter-model relationship between base-climate sea ice climatology and 21st-century AA: Relationship between (a) SIE and AA ($r = -0.70$), (b) SIC and AA ($r = -0.77$), and (c) sea ice seasonality ($SIC_{FMA} - SIC_{JAS}$) and AA ($r = 0.73$). All correlations are statistically significant at the 95% level. All values except for $SIC_{FMA} - SIC_{JAS}$ represent annual means. Each model is denoted by a circle, color coded by the degree of AA (corresponding to y-axes). The mean observational estimate (2016–2022) for each sea ice metric is shown by the grey dotted line, with grey shaded areas giving ± 1 of the inter-annual standard deviation. The gray bar along the y-axes gives the standard deviation around the constrained future projection.

apply a hierarchical statistical framework (Bowman *et al* 2018) to derive the mean and standard deviation of each constrained future projection. We then calculate the constrained range of future AA by deriving the mean Gaussian distribution from the three predictors. The 95% prediction interval of the 21st-century AA is quantified by 2.47–3.34.

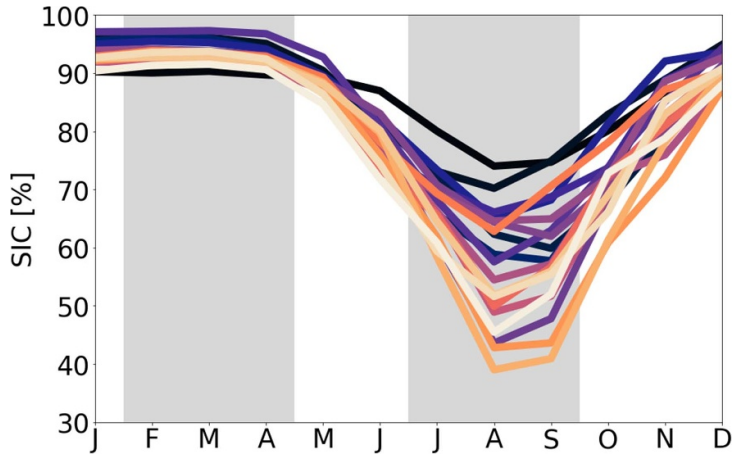

Figure 4. Sea ice seasonality: seasonal cycle of base-climate, monthly SIC. Each line accounts for one model, color coded by the degree of AA (corresponding to figure 3). To derive the model-specific seasonality, we calculate the difference between the mean SIC during FMA and JAS (marked by shaded areas, with values corresponding to figure 3(c)).

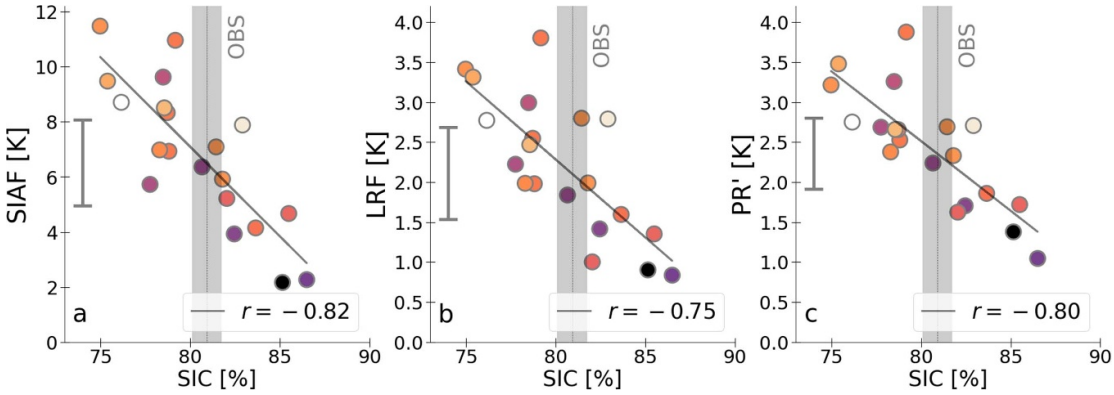

Figure 5. Inter-model relationship between base-climate SIC and end-of-century climate feedbacks: Relationship between (a) SIC and SIAF ($r = -0.82$), (b) SIC and LRF ($r = -0.75$), and (c) SIC and PR' ($r = -0.80$). All correlations are statistically significant at the 95% level. Climate feedbacks are expressed as a warming contribution to the total Arctic warming at the end of the century. All values represent annual means. Each model is denoted by a circle, color coded by the degree of AA (corresponding to figure 3). The mean observational estimate (2016–2022) for SIC is shown by the grey dotted line, with grey shaded areas giving ± 1 of the inter-annual standard deviation. The gray bar along the y-axes gives the standard deviation around the constrained future projection.

3.4. The role of climate feedbacks

To further explore the physical underpinnings of the systematic links between observable sea-ice metrics and the future evolution of AA, we compute the warming contribution of climate feedbacks that strongly mediate AA. Each of the individual climate feedbacks in figure 5 (SIAF, LRF, and PR', respectively) shows the strongest correlation with the base-climate SIC (relative to the other sea ice metrics in figure 3; not shown). All feedbacks show negative significant correlations with the current climate's SIC. In particular, models with a lower SIC in the base climate project larger feedback contributions to the total Arctic warming at the end of the century. These models simultaneously simulate a larger AA in the future. The SIAF shows the largest warming contribution across all models, and a strong link to the base-climate SIC (figure 5(a); $r = -0.82$), which is due to the strong correlation of long-term SIC and albedo changes ($r = 0.86$; not shown). Also for the LRF and PR', the relationships to the base-climate SIC are significant, with $r = -0.75$ (figure 5(b)) and $r = -0.80$ (figure 5(c)), respectively.

On the basis of figure 5 we compute the 95% prediction interval of each feedback's warming contribution to the end-of-century Arctic warming (2070–2099) with 3.96–9.08 K for the SIAF, 1.16–3.06 K for the LRF, and 1.62–3.09 K for the PR', respectively.

4. Discussion

We have derived significant linear relationships between current-climate sea ice amount and seasonality, and future AA across an ensemble of CMIP6 models under a high emission scenario. In particular, it is shown

that the magnitude of future AA is negatively correlated with SIE and area-average SIC in the base climate, and positively correlated with the intensity of the sea-ice seasonal cycle.

We propose an EC on future AA from the derived relationships to the sea ice climatology, in conjunction with satellite observations. Previous studies have highlighted the importance of confirming that emerging relationships have physical underpinnings along with their statistical robustness (Hall *et al* 2019). Already earlier work has shown a causal link between the inter-model difference in sea-ice loss and its initial state (Massonnet *et al* 2018, Bonan *et al* 2021). Furthermore, it has been shown that the degree of recent Arctic temperature amplification can be traced back to the intensity of sea ice loss (Screen and Simmonds 2010, Dai *et al* 2019) and, further, that related climate feedbacks that drive AA correlate with the seasonal melt signal across models (Thackeray and Hall 2019).

We suggest the current-climate sea ice state as an appropriate predictor for the magnitude of future AA by setting the stage for long-term climatological changes: A lower base-climate SIE systematically relates to a lower percentage of sea ice covering the Arctic ocean, relative to a larger projected SIE. We propose that the Arctic-mean SIC is the key factor at play, both in an annual-mean and seasonal context of the current climate:

Firstly, an ice cover with lower SIC is more prone to further ice loss through the 21st century, which links to relevant climate feedbacks at play (Hall 2004, Soden and Held 2006, Graversen *et al* 2014, Pithan and Mauritsen 2014, Feldl *et al* 2020), and ultimately leads to a stronger future AA. In this context, we explicitly show that each of the feedbacks that are known contributors to AA (SIAF, LRF, and PR') are systematically related to the initial sea ice amount: Models with a lower base-climate SIC project a stronger feedback warming contribution to the total Arctic warming in the future. We argue that the positive relationship between base-climate SIC and its long-term changes is linked to the negative SIC-SIAF relationship, and further, that temperature feedbacks (LRF and PR') play a role: A lower base-climate SIC sets the stage for both additional ice melt and surface warming through a stronger SIAF and temperature feedbacks, respectively, which ultimately adds to AA in the future.

Secondly, the larger tendency for long-term sea ice loss in the low-SIC models further reflects in the intensity of seasonal ice melt and subsequent refreeze: Models with lower SIC project a larger seasonality as a measure between ice maximum (during FMA) and minimum (during JAS), compared to models with higher SIC. These models hence show a higher potential of seasonal redistribution of heat, from May–September when the ocean opens up and draws energy from atmosphere via solar absorption, to October–April when the ocean acts as heat source for the colder atmosphere via outgoing long-wave radiation and turbulent heat fluxes (Holland and Bitz 2003, Boeke and Taylor 2018, Feldl *et al* 2020, Linke and Quaas 2022). Our results confirm that models with larger seasonality in the current climate systematically produce a stronger AA in the future.

The derived relationships are sensitive to a sub-selection of models from the entire ensemble of 30 CMIP6 models. By excluding 10 models that project the lowest SIC in the current climate, we derive the strongest linear relationships. We justify the model exclusion following Thackeray and Hall (2019), who exclude models with the lowest historical sea-ice thickness to constrain the climatological SIAF in CMIP5. We argue that these models project a base-climate sea ice amount that is too low to follow the linear relationship between base-climate SIC and its long-term changes (figure B1(b)): According to the linear SIC-d SIC relationship, models below an average SIC of approximately 75% would have to project a future ice loss of approximately 100% or more. We understand the strong link between initial sea ice amount and future sea ice loss as a necessary condition to establish an EC on future AA based on the current-climate sea ice: AA largely decreases when sea ice melts away completely, and the inter-model spread in AA projections can be traced back to a variable projection of sea-ice loss across climate models (Dai *et al* 2019). It can therefore be expected that the inclusion of models that are below a certain threshold of initial sea ice amount leads to a break down of emerging relationships: For those simulations, the impact of sea ice changes on AA has decreased substantially given its low initial amount. We thereby justify the removal of those models that do not follow the required linear relationship (SIC-d SIC) under a high emission scenario. However, even with all 30 models included (as shown in figure C1), the EC on future AA lies within the same range as for the sub-selected ensemble (2.29–3.33), albeit slightly smaller than the main prediction. The smaller magnitude in AA when including the lowest-SIC models in the base climate is an expected result, since the ice-free state is reached early on in the century in those simulations (figure 1), which dampens the effect of long-term ice loss on AA.

In addition, the strength of emerging relationships is sensitive to the choice of base period and thereby the prediction interval for the 21st-century AA. The base period of 2005–2034 is chosen as a compromise between establishing sufficiently strong relationships and including enough observations. To justify the use of the model base period that partly includes future years and is thereby not entirely covered by the observations, we compare the average sea ice metrics during 2005–2034 against the corresponding averages for 2016–2022 (observational base period) in the model output. We derive strong linear relationships of

$r = 0.99$, $r = 0.86$ and $r = 0.91$ for SIE, SIC and seasonal SIC, respectively, and a cosine distance (as a measure of similarity) below 0.005 for all metrics (not shown). The strong similarity between averaged sea ice metrics for 2005–2034 and 2016–2022 in the simulated data set can justify the choice of base period.

We further test the sensitivity of our results to the choice of base period, and select as alternative an earlier period that covers the entire range of observations. By choosing a base period of e.g. 2008–2022, the relationships to future AA degrade ($r = -0.67$, $r = -0.68$ and $r = 0.72$ for SIE, SIC and seasonality, respectively, not shown). We expect that the relationship weakening by moving the base period into the past is merely statistical, i.e. the inter-model spread in historical sea ice metrics is smaller compared to the future scenarios. However, the relationships are still strong enough to manifest the physical underpinnings of this study, i.e. the connection between sea ice climatology, future ice loss and AA. Furthermore, the AA prediction interval (2.53–3.47) is close to the one based on 2005–2034.

From the combination of ECs derived for all appropriate predictors (SIE, SIC, and sea-ice seasonal cycle), we derive a prediction interval for AA of 2.47–3.34. We note that our constraint gives an estimate of the mean local amplification over the base-climate sea ice cover. We thereby exclude open Arctic ocean and land masses within the NH66 domain, respectively. Including open ocean expectedly weakens the linear relationships and the constrained future prediction decreases to 2.08–2.74.

In addition to predicting the future evolution of AA through the 21st century, we propose a constraint on the first year of a seasonally ice-free Arctic. Previous studies give a prediction interval on the Arctic's ice-free timing under high emission scenarios: Massonnet *et al* (2012) predict an ice-free Arctic during summer for 2041–2060 based on historical sea ice in CMIP5. For CMIP6, Bonan *et al* (2021) predict that the Arctic Ocean will likely be ice free in September 2036–2056. Notz and SIMIP Community (2020) show that in most CMIP6 simulations, an ice-free September occurs for the first time before 2050 under low, intermediate and high emission scenarios. Recent findings of Kim *et al* (2023) confirm that the Arctic is projected to be seasonally ice-free in the next decade or two, irrespective of emission scenarios in CMIP6. Our constraint is based on the tight relationship between base-climate SIC and the ice-free timing across CMIP6 models. The prediction interval (2038–2059) lies well in the range of previous estimates, which further strengthens the prediction of a seasonally ice-free Arctic by mid-century.

Lastly, our results from the highest emission scenario suggest that AA is expected to continue at a rate more than twice as global average, even under the likelihood of seasonally ice-free conditions by mid-century. However, AA is unlikely to be as strong as in the early 2000s, where a peak value has been identified contemporaneous with a peak in sea ice loss (Davy and Griewank 2023). Again, this concurrent occurrence of peaking AA and sea ice loss hints to the crucial role of ice melt for the evolution of AA, and further suggests that if sea ice melts away entirely, the sea-ice control on the evolution of AA diminishes. Thereby, our established relationships are expected to break down eventually with time.

5. Conclusion

Arctic sea ice loss is a major driver of AA, and the variable degree in future sea ice projections across climate models is linked to the spread in contemporaneous AA magnitude. We argue that the variable model projections in ice loss through the 21st century are a consequence of the sea ice amount in the current climate. The implication is that the current climate's sea ice climatology systematically links to the magnitude of future AA, and is thereby an appropriate predictor for future Arctic climate change. We capture the strongest emerging relationship for the Arctic-mean SIC which gives an estimate of the fraction by which the Arctic ocean is currently covered by sea ice. In particular, CMIP6 models with a lower base-climate SIC predict a stronger future AA through setting the stage for larger ice melt in both future climate and seasonal cycle, which links to the relevant feedbacks at play. These results justify the conclusion that the base-climate sea ice climatology across models at least partly explains the inter-model spread in future Arctic climate projection.

The combination of our derived ECs gives a prediction interval of future Arctic warming that is amplified by a factor of 2.47–3.34 as compared to the global-average warming. This implies that the modern era of AA starting from the end of the 20th century (Overland *et al* 2008, Serreze and Barry 2011, Wendisch *et al* 2023) will continue through the 21st century, and possibly beyond. Lastly, the simulated timing of an ice-free Arctic in September is sensitive to the current-climate sea ice amount, which leads to the prediction of a seasonally ice-free Arctic around mid-century under a high emission scenario, in accordance with previous studies.

Data availability statement

CMIP6 data was provided by the DKRZ (Deutsches Klimarechenzentrum; https://esgf-data.dkrz.de/search/cmip6-dkrz/.

Sea ice concentration data is provided by the European Organisation for the Exploitation of Meteorological Satellites (EUMETSAT) Ocean and Sea Ice Satellite Application Facility (OSI SAF), and can be downloaded from the Climate Data Store (https://doi.org/10.24381/cds.3cd8b812) (Copernicus Climate Change Service (C3S) 2020). All data that support the findings of this study are included within the article (and any supplementary information files).

Acknowledgment

We gratefully acknowledge the funding by the Deutsche Forschungsgemeinschaft (DFG, German Research Foundation)—Grant No. 268020496–TRR 172, within the Transregional Collaborative Research Center 'ArctiC Amplification: Climate Relevant Atmospheric and SurfaCe Processes, and Feedback Mechanisms', $(AC)^3$. Funding is further acknowledged from the EU Horizon 2020 project 'CONSTRAIN' (GA No. 820829) and National Science Foundation Award AGS-1753034. We acknowledge the World Climate Research Programme which coordinated and promoted CMIP6. We thank the climate modelling groups for producing and making available their model output, the Earth System Grid Federation (ESGF) for archiving the data and providing access, and the multiple funding agencies who support CMIP6 and ESGF. The authors would like to thank Julien Lenhardt for discussing and revising this paper.

Appendix A. Inter-model spread in AA

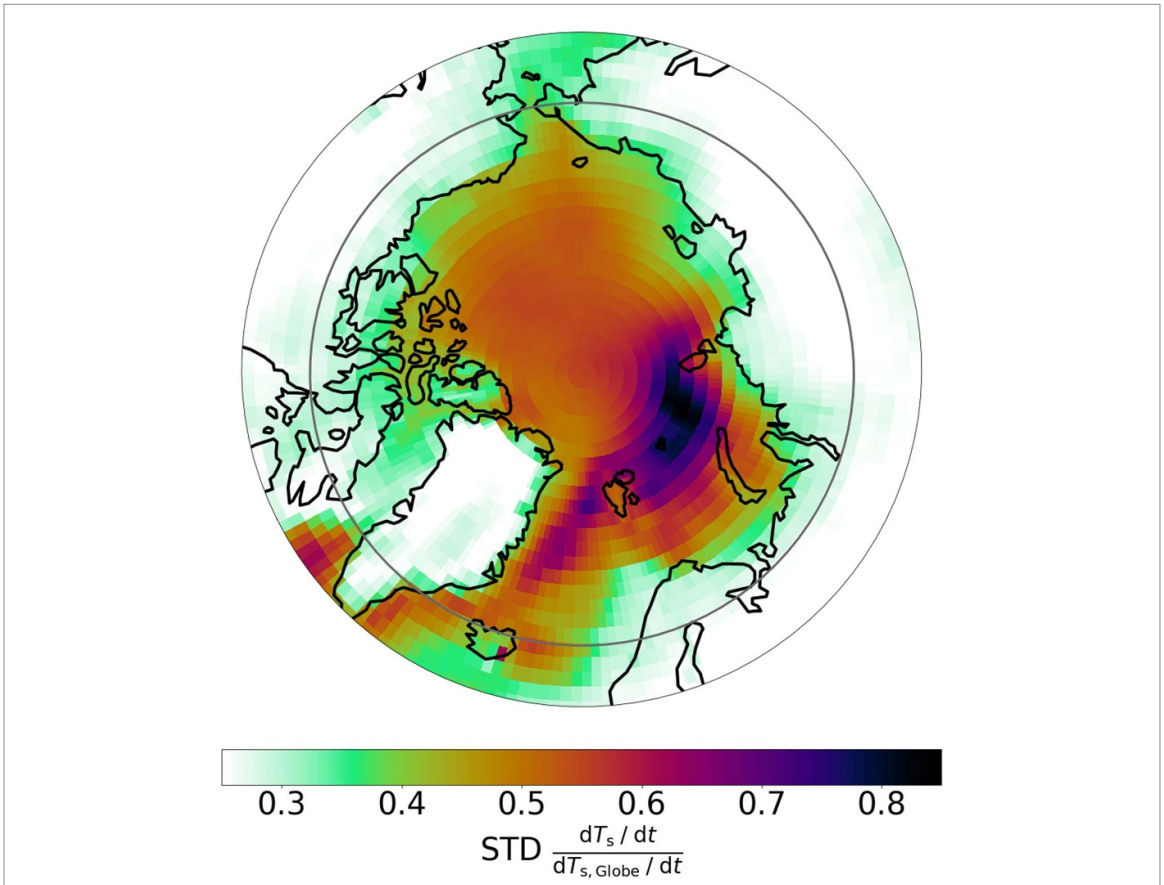

Figure A1. Inter-model standard deviation (STD) across 20 CMIP6 models corresponding to figure 2.

Appendix B. Long-term and seasonal sea ice loss

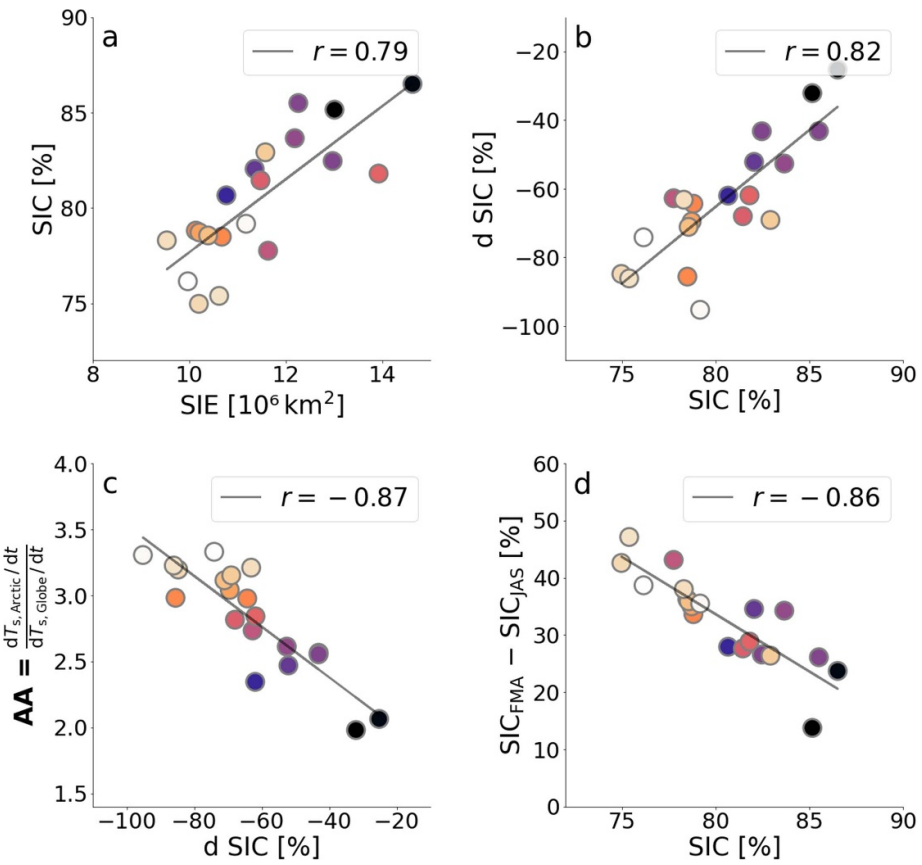

Figure B1. Inter-model relationships across CMIP6 models: Relationship between (a) base-climate SIE and SIC ($r = 0.79$), (b) base-climate SIC and its long-term changes (d SIC; derived from the linear trend in SIC 2005–2099; $r = 0.82$), (c) d SIC and future AA ($r = -0.87$), and (d) base-climate SIC and $SIC_{FMA} - SIC_{JAS}$ ($r = -0.86$). All correlations are statistically significant at the 95% level. All values except for $SIC_{FMA} - SIC_{JAS}$ represent annual means. Each model is denoted by a circle, color coded by the degree of AA (corresponding to *y*-axis in panel (c)).

Appendix C. Emergent constraint for all 30 models

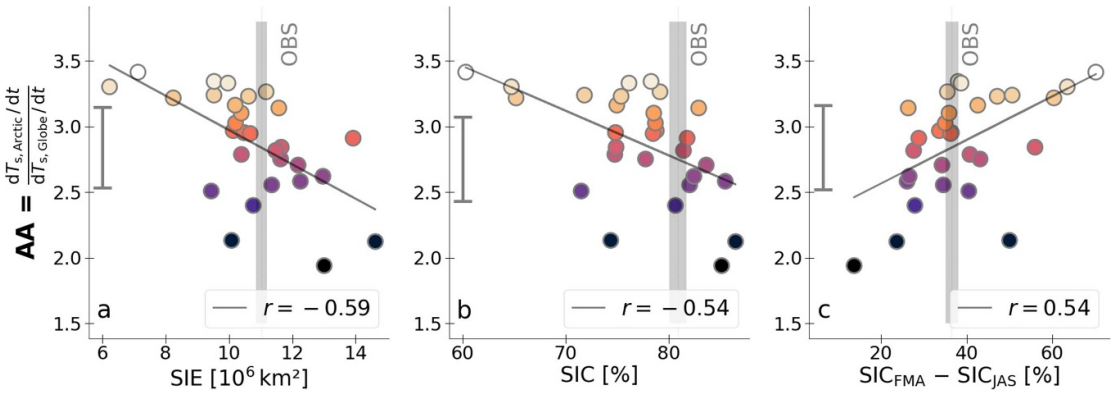

Figure C1. Same as figure 3, but with all 30 CMIP6 models listed in table 1: Relationship between (a) SIE and AA ($r = -0.59$), (b) SIC and AA ($r = -0.54$), and (c) sea-ice seasonality ($SIC_{FMA} - SIC_{JAS}$) and AA ($r = 0.54$). All correlations are statistically significant at the 95% level.

ORCID iDs

Olivia Linke https://orcid.org/0000-0002-5286-2185
Nicole Feldl https://orcid.org/0000-0002-2631-1419
Johannes Quaas https://orcid.org/0000-0001-7057-194X

References

Bentsen M *et al* 2019 NCC NorESM2-MM model output prepared for CMIP6 ScenarioMIP *Earth System Grid Federation* (https://doi.org/10.22033/ESGF/CMIP6.608)
Block K and Mauritsen T 2013 *J. Adv. Model. Earth Syst.* **5** 676–91
Boeke R C and Taylor P C 2018 *Nat. Commun.* **9** 5017
Bonan D B, Schneider T, Eisenman I and Wills R C 2021 *Geophys. Res. Lett.* **48** e2021GL094309
Boucher O *et al* 2019 IPSL IPSL-CM6A-LR model output prepared for CMIP6 ScenarioMIP *Earth System Grid Federation* (https://doi.org/10.22033/ESGF/CMIP6.1532)
Bowman K W, Cressie N, Qu X and Hall A 2018 *Geophys. Res. Lett.* **45** 050–13,059
Cao J 2019 NUIST NESMv3 model output prepared for CMIP6 ScenarioMIP *Earth System Grid Federation* (https://doi.org/10.22033/ESGF/CMIP6.2027)
Cohen J *et al* 2014 *Nat. Geosci.* **7** 627–37
Copernicus Climate Change Service (C3S) 2020 Sea ice concentration daily gridded data from 1979 to present derived from satellite observations Copernicus Climate Change Service (C3S) Climate Data Store (CDS) (https://doi.org/10.24381/cds.3cd8b812) (Accessed 2 February 2023)
Dai A, Luo D, Song M and Liu J 2019 *Nat. Commun.* **10** 21
Danabasoglu G 2019 NCAR CESM2 model output prepared for CMIP6 ScenarioMIP *Earth System Grid Federation* (https://doi.org/10.22033/ESGF/CMIP6.2201)
Davy R and Griewank P 2023 *Environ. Res. Lett.* **18** 084003
Dix M *et al* 2019 CSIRO-ARCCSS ACCESS-CM2 model output prepared for CMIP6 ScenarioMIP *Earth System Grid Federation* (https://doi.org/10.22033/ESGF/CMIP6.2285)
EC-Earth Consortium 2019 EC-Earth-Consortium EC-Earth3 model output prepared for CMIP6 ScenarioMIP *Earth System Grid Federation* (https://doi.org/10.22033/ESGF/CMIP6.251)
EC-Earth Consortium 2019 EC-Earth-Consortium EC-Earth3-Veg model output prepared for CMIP6 ScenarioMIP *Earth System Grid Federation* (https://doi.org/10.22033/ESGF/CMIP6.727)
EC-Earth Consortium 2020 EC-Earth-Consortium EC-Earth3-Veg-LR model output prepared for CMIP6 ScenarioMIP *Earth System Grid Federation* (https://doi.org/10.22033/ESGF/CMIP6.728)
EC-Earth Consortium 2021 EC-Earth-Consortium EC-Earth3-CC model output prepared for CMIP6 ScenarioMIP *Earth System Grid Federation* (https://doi.org/10.22033/ESGF/CMIP6.15327)
Feldl N, Po-Chedley S, Singh H K, Hay S and Kushner P J 2020 *npj Clim. Atmos. Sci.* **3** 41
Feldl N and Roe G 2013 *Geophys. Res. Lett.* **40** 4007–11
Francis J A, Vavrus S J and Cohen J 2017 *Wiley Interdiscip. Rev. Clim. Change* **8** e474
Good P 2019 MOHC HadGEM3-GC31-LL model output prepared for CMIP6 ScenarioMIP *Earth System Grid Federation* (https://doi.org/10.22033/ESGF/CMIP6.10845)
Good P, Sellar A, Tang Y, Rumbold S, Ellis R, Kelley D, Kuhlbrodt T and Walton J 2019 MOHC UKESM1.0-LL model output prepared for CMIP6 ScenarioMIP *Earth System Grid Federation* (https://doi.org/10.22033/ESGF/CMIP6.1567)
Goosse H *et al* 2018 *Nat. Commun.* **9** 1–13
Graversen R G, Langen P L and Mauritsen T 2014 *J. Clim.* **27** 4433–50
Guo H *et al* 2018 NOAA-GFDL GFDL-CM4 model output prepared for CMIP6 ScenarioMIP *Earth System Grid Federation* (https://doi.org/10.22033/ESGF/CMIP6.9242)
Hahn L C, Armour K C, Zelinka M D, Bitz C M and Donohoe A 2021 *Front. Earth Sci.* **9** 710036
Hall A 2004 *J. Clim.* **17** 1550–68
Hall A, Cox P, Huntingford C and Klein S 2019 *Nat. Clim. Change* **9** 269–78
Holland M M and Bitz C M 2003 *Clim. Dyn.* **21** 221–32
Huang W 2019 THU CIESM model output prepared for CMIP6 ScenarioMIP *Earth System Grid Federation* (https://doi.org/10.22033/ESGF/CMIP6.1357)
Huguenin M F, Holmes R M and England M H 2022 *Nat. Commun.* **13** 4921
Jackson L 2020 MOHC HadGEM3-GC31-MM model output prepared for CMIP6 ScenarioMIP *Earth System Grid Federation* (https://doi.org/10.22033/ESGF/CMIP6.10846)
John J G *et al* 2018 NOAA-GFDL GFDL-ESM4 model output prepared for CMIP6 ScenarioMIP *Earth System Grid Federation* (https://doi.org/10.22033/ESGF/CMIP6.1414)
Kim Y H, Min S K, Gillett N P, Notz D and Malinina E 2023 *Nat. Commun.* **14** 3139
Klein S and Hall A 2015 *Curr. Clim. Change Rep.* **1** 276–87
Lavergne T *et al* 2019 *Cryosphere* **13** 49–78
Linke O and Quaas J 2022 *Tellus* A **74** 106–18
Lovato T and Peano D 2020 CMCC CMCC-CM2-SR5 model output prepared for CMIP6 ScenarioMIP *Earth System Grid Federation* (https://doi.org/10.22033/ESGF/CMIP6.1365)
Lovato T, Peano D and Butenschön M 2021 CMCC CMCC-ESM2 model output prepared for CMIP6 ScenarioMIP *Earth System Grid Federation* (https://doi.org/10.22033/ESGF/CMIP6.13168)
Massonnet F, Fichefet T, Goosse H, Bitz C M, Philippon-Berthier G, Holland M M and Barriat P Y 2012 *Cryosphere* **6** 1383–94
Massonnet F, Vancoppenolle M, Goosse H, Docquier D, Fichefet T and Blanchard-Wrigglesworth E 2018 *Nat. Clim. Change* **8** 599–603
NASA/GISS 2020 NASA-GISS GISS-E2.1G model output prepared for CMIP6 ScenarioMIP *Earth System Grid Federation* (https://doi.org/10.22033/ESGF/CMIP6.2074)
Notz D SIMIP Community 2020 *Geophys. Res. Lett.* **47** e2019GL086749
O'Neill B C *et al* 2016 *Geosci. Model Dev.* **9** 3461–82

Overland J E, Dethloff K, Francis J A, Hall R J, Hanna E, Kim S J, Screen J A, Shepherd T G and Vihma T 2016 *Nat. Clim. Change* **6** 992–9
Overland J, Wang M and Salo S 2008 *Tellus* A **60** 589–97
Pithan F and Mauritsen T 2014 *Nat. Geosci.* **7** 181–4
Polyakov I V, Walsh J E and Kwok R 2012 *Bull. Am. Meteorol. Soc.* **93** 145–51
Rantanen M, Karpechko A Y, Lipponen A, Nordling K, Hyvärinen O, Ruosteenoja K, Vihma T and Laaksonen A 2022 *Commun. Earth Environ.* **3** 1–10
Rong X 2019 CAMS CAMS-CSM1.0 model output prepared for CMIP6 ScenarioMIP *Earth System Grid Federation* (https://doi.org/10.22033/ESGF/CMIP6.11004)
Schupfner M *et al* 2019 DKRZ MPI-ESM1.2-HR model output prepared for CMIP6 ScenarioMIP *Earth System Grid Federation* (https://doi.org/10.22033/ESGF/CMIP6.2450)
Screen J A and Simmonds I 2010 *Nature* **464** 1334–7
Seland Ø *et al* 2019 NCC NorESM2-LM model output prepared for CMIP6 ScenarioMIP *Earth System Grid Federation* (https://doi.org/10.22033/ESGF/CMIP6.604)
Serreze M C and Barry R G 2011 *Glob. Planet. Change* **77** 85–96
Serreze M C and Francis J A 2006 *Clim. Change* **76** 241–64
Serreze M, Barrett A, Stroeve J, Kindig D and Holland M 2009 *Cryosphere* **3** 11–19
Smith C J, Kramer R J and Sima A 2020 *Earth Syst. Sci. Data* **12** 2157–68
Smith D M *et al* 2019 *Geosci. Model Dev.* **12** 1139–64
Soden B J and Held I M 2006 *J. Clim.* **19** 3354–60
Song Z, Qiao F, Bao Y, Shu Q, Song Y and Yang X 2019 FIO-QLNM FIO-ESM2.0 model output prepared for CMIP6 ScenarioMIP *Earth System Grid Federation* (https://doi.org/10.22033/ESGF/CMIP6.9051)
Stroeve J C, Kattsov V, Barrett A, Serreze M, Pavlova T, Holland M and Meier W N 2012 *Geophys. Res. Lett.* **39** 16
Swart N C *et al* 2019 CCCma CanESM5 model output prepared for CMIP6 ScenarioMIP *Earth System Grid Federation* (https://doi.org/10.22033/ESGF/CMIP6.1317)
Swart N C *et al* 2019 CCCma CanESM5-CanOE model output prepared for CMIP6 ScenarioMIP *Earth System Grid Federation* (https://doi.org/10.22033/ESGF/CMIP6.10207)
Tachiiri K *et al* 2019 MIROC MIROC-ES2L model output prepared for CMIP6 ScenarioMIP *Earth System Grid Federation* (https://doi.org/10.22033/ESGF/CMIP6.936)
Taylor P C, Cai M, Hu A, Meehl J, Washington W and Zhang G J 2013 *J. Clim.* **26** 7023–43
Thackeray C W and Hall A 2019 *Nat. Clim. Change* **9** 972–8
Voldoire A 2019 CNRM-CERFACS CNRM-CM6-1 model output prepared for CMIP6 ScenarioMIP *Earth System Grid Federation* (https://doi.org/10.22033/ESGF/CMIP6.1384)
Voldoire A 2019 CNRM-CERFACS CNRM-CM6-1-HR model output prepared for CMIP6 ScenarioMIP *Earth System Grid Federation* (https://doi.org/10.22033/ESGF/CMIP6.1388)
Wang M and Overland J E 2012 *Geophys. Res. Lett.* **39** L18501
Wendisch M *et al* 2023 *Bull. Am. Meteorol. Soc.* **104** E208–42
Xin X, Wu T, Shi X, Zhang F, Li J, Chu M, Liu Q, Yan J, Ma Q and Wei M 2019 BCC BCC-CSM2MR model output prepared for CMIP6 ScenarioMIP *Earth System Grid Federation* (https://doi.org/10.22033/ESGF/CMIP6.1732)
Yukimoto S *et al* 2019 MRI MRI-ESM2.0 model output prepared for CMIP6 ScenarioMIP *Earth System Grid Federation* (https://doi.org/10.22033/ESGF/CMIP6.638)
Ziehn T *et al* 2019 CSIRO ACCESS-ESM1.5 model output prepared for CMIP6 ScenarioMIP *Earth System Grid Federation* (https://doi.org/10.22033/ESGF/CMIP6.2291)